ADVANCED FUNCTIONAL MATERIALS

Supporting Information

for *Adv. Funct. Mater.,* DOI: 10.1002/adfm.201801380

Thin, Millimeter Scale Fingernail Sensors for Thermal Characterization of Nail Bed Tissue

Yajing Li, Yinji Ma, Chen Wei, Haiwen Luan, Shuai Xu, Mengdi Han, Hangbo Zhao, Cunman Liang, Quansan Yang, Yiyuan Yang, Kaitlyn E. Crawford, Xue Feng, Yonggang Huang, and John A. Rogers**

DOI: 10.1002/ ((adfm.201801380))
Article type: Full Paper

Supporting Information

Thin, Millimeter Scale Fingernail Sensors for Thermal Characterization of Nail Bed Tissue

Yajing Li, Yinji Ma, Chen Wei, Haiwen Luan, Shuai Xu, Mengdi Han, Hangbo Zhao, Cunman Liang, Quansan Yang, Yiyuan Yang, Kaitlyn E. Crawford, Xue Feng, Yonggang Huang, John A. Rogers**

Dr. Y. Li

Department of Materials Science and Engineering, Center for Bio-Integrated Electronics

Northwestern University

Evanston, IL 61801, USA

Dr. Y. Ma, Prof. X. Feng

Department of Engineering Mechanics; Center for Mechanics and Materials

Tsinghua University

Beijing, 100084, China

C. Wei, H. Luan

Department of Civil and Environmental Engineering, Mechanical Engineering, Materials Science and Engineering

Northwestern University

Evanston, IL, 60208, USA

Dr. S. Xu

Center for Bio-Integrated Electronics, Department of Dermatology, Feinberg School of Medicine

Northwestern University

Evanston, IL 60208, USA

Dr. M. Han, Dr. H. Zhao, C. Liang, Q. Yang, Y. Yang

Center for Bio-Integrated Electronics, Northwestern University

Evanston, IL 60208, USA

Prof. K. E. Crawford

Department of Materials Science and Engineering, Burnett School of Biomedical Sciences

University of Central Florida

Orlando, FL 32827, USA

[*] Prof. Y. Huang, Corresponding Author

Department of Civil and Environmental Engineering, Mechanical Engineering, Materials Science and Engineering, Skin Disease Research Center, Feinberg School of Medicine

Northwestern University

Evanston, IL, 60208, USA

Email: y-huang@northwestern.edu

[*] Prof. J. A. Rogers, Corresponding Author

Departments of Materials Science and Engineering, Biomedical Engineering, Chemistry, Mechanical Engineering, Electrical Engineering and Computer Science, and Neurological Surgery

Center for Bio-Integrated Electronics

Simpson Querrey Institute for Nano/biotechnology

Northwestern University

Evanston, IL 60208, USA

Email: jrogers@northwestern.edu

Keywords: thermal sensor, flexible devices, fingernail devices, non-invasive tissue characterization, perfusion tracking

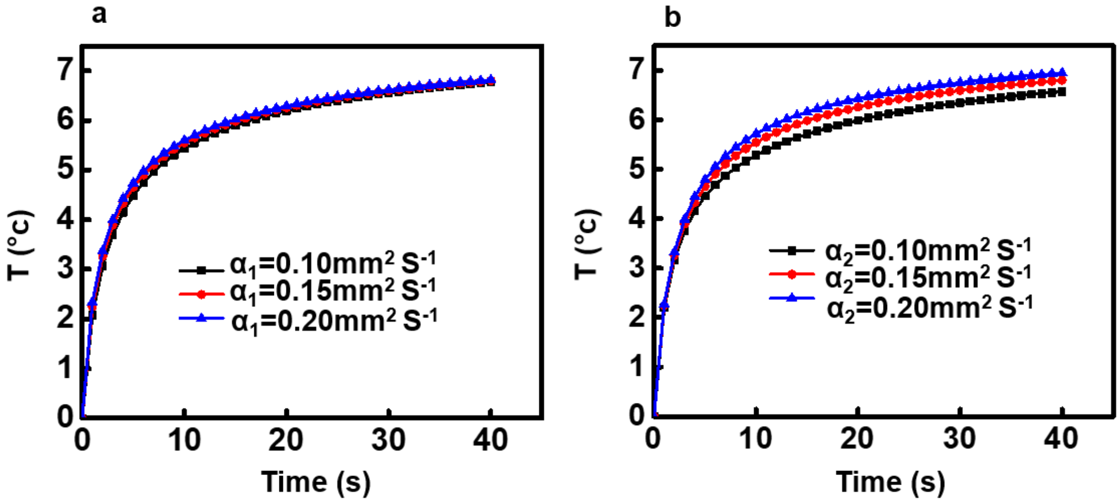

Figure S1 Thermal diffusivity influence in the FEA simulation. FEA simulated temperature curves of R=1.5mm sensor. Parameters adopted in the simulations are: (a)top layer thickness h=0.3 mm, power q=3 mw mm^{-2}, thermal conductivity of top layer k_1=0.24 W $m^{-1}K^{-1}$, thermal conductivity of bottom layer k_2=0.55W $m^{-1}K^{-1}$. Thermal diffusivity of top layer α_1=0.1 mm^2 s^{-1}(black),0.15 mm^2 s^{-1} (red),0.2 mm^2 s^{-1} (blue), thermal diffusivity of bottom layer α_2=0.15 mm^2 s^{-1}. (b) α_1=0.15 mm^2 s^{-1}, α_2=0.1 mm^2 s^{-1} (black),0.15 mm^2 s^{-1} (red),0.2 mm^2 s^{-1} (blue).

To evaluate the influence of the thermal diffusivity in the FEA simulations, temperature rise curve of R=1.5 mm sensor is calculated according to different values of thermal diffusivity of top and bottom materials. Calculation results in **Figure S1** reveal the sensitivity of computed results on those two parameters, corresponding to the case of representative data from human nail plate[1] and skin[2]. The study involves systematically increasing the value of α_1 (0.10 mm^2 s^{-1}) by 50%, 100%, and fixing this value and recalculating the data while allowing only α_2 to change. For 100% change of thermal diffusivity of top layer material, steady state temperature of the sensor at 40s does not change significantly in Figure S1a. Variation of the thermal diffusivity of bottom layer leads to ± 3% difference of the steady temperature in Figure S 1b, suggesting the fitting results has a weak dependence of thermal diffusivity α.

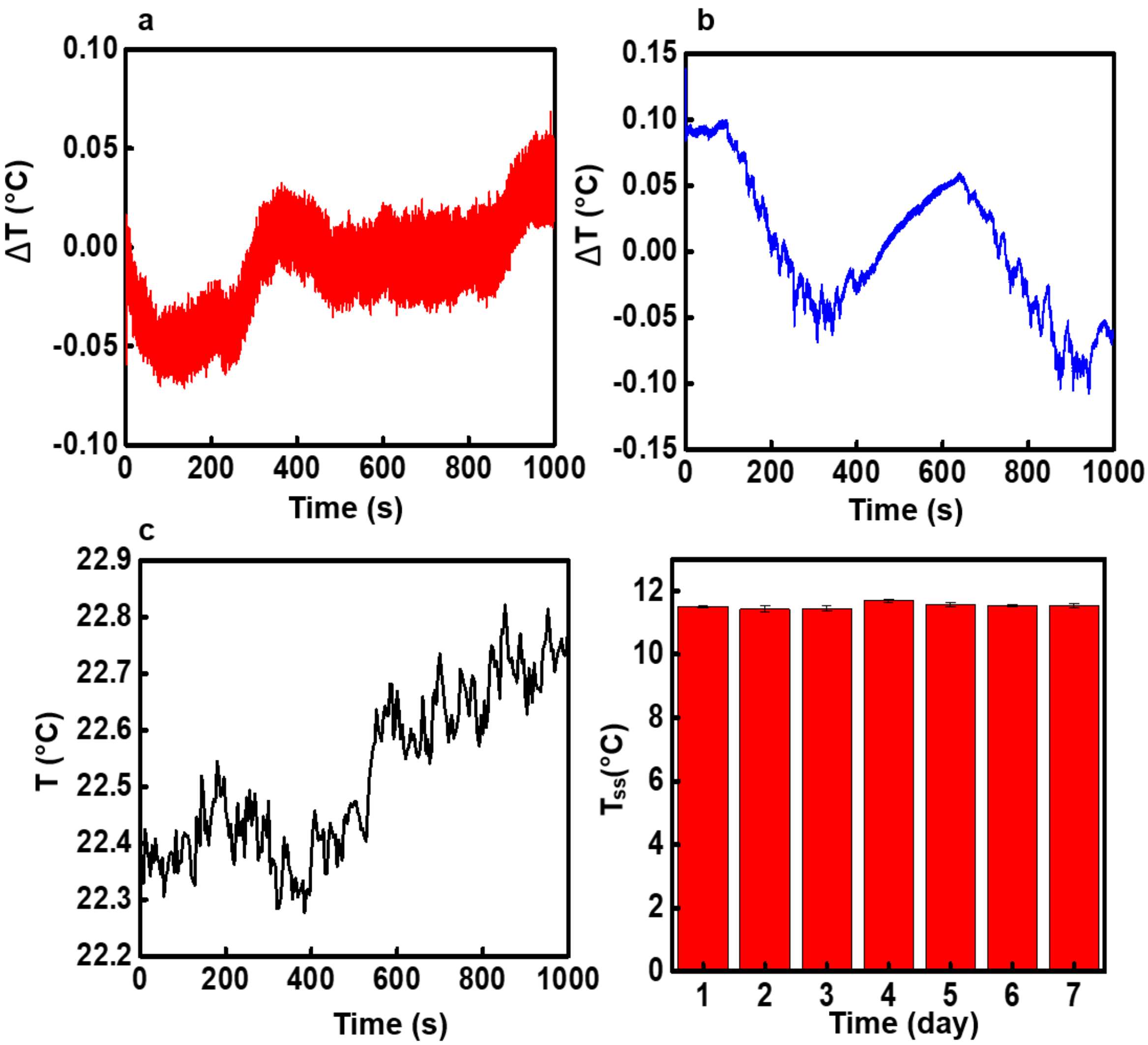

Figure S2 Fluctuations in ambient temperature. (a) Temperature measured using a sensor with R=1.5 mm on Sylgard170 with a petri dish enclosure. (b) Temperature measured using a sensor with R=1.5 mm on Sylgard170 with a plastic foam enclosure. (c) Temperature of Sylgard170 recorded by an infrared camera without the petri dish enclosure. (d) Steady state temperature of a sensor with R=1.5 mm on Ecoflex measured over a period of 7 days with a plastic foam enclosure.

Figure S2a summarizes measurements of the fluctuations in temperature measured from a sensor with R=1.5 mm on Sylgard170. The variations are smaller than 0.1 °C. Figure S2b shows similar measurements but performed with a piece of plastic foam as an enclosure identical to the one used for measurements on human subjects. For the images and data in Figure S2c, the infrared camera was focused on the Sylgard170 without the petri dish enclosure and each data point represents a temperature value averaged over the area enclosed by a circle with radius 1.5 mm. The measurements show a 0.5 °C variation in temperature during 15 min. Figure S2d summarizes data on the long-term stability of the sensor response for measurements on a piece of Ecoflex with a plastic foam enclosure over 7 days. The magnitude of the variations in temperature are ±0.1 °C, comparable to those shown in (b).

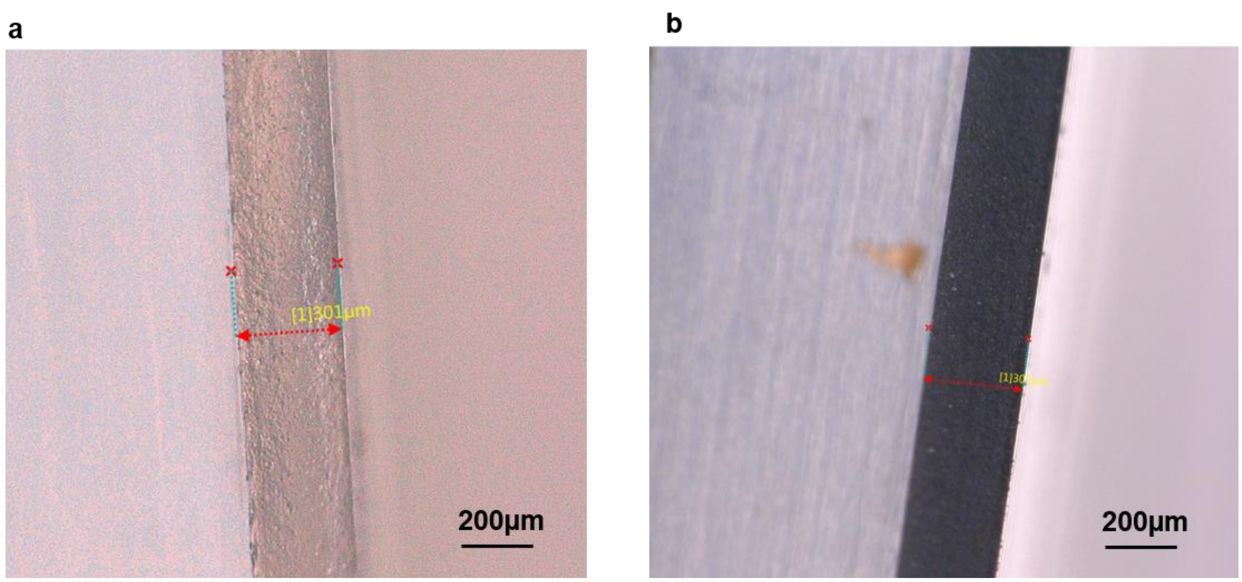

Figure S3. Optical images of the cross-section of the top film in the bi-layer model. (a) Ecoflex with thickness of 300 μm (b) Sylgard 567 with thickness of 300 μm.

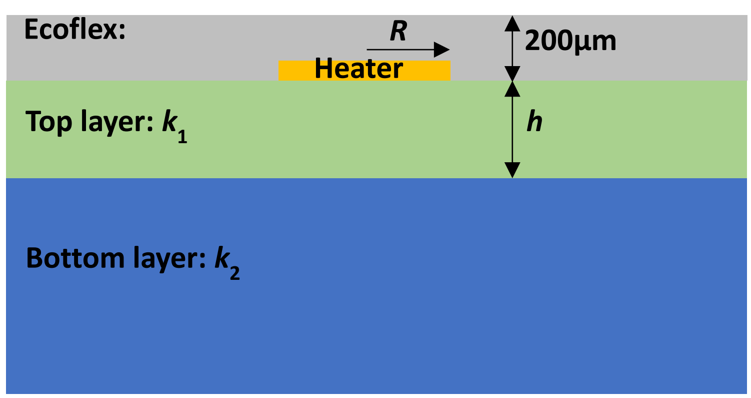

Figure S4. Schematic diagram of the analytical model in the FEA simulation. A round heater (radius, R), covered by 200 um Ecoflex encapsulation layer, is placed on a bi-layer sample with top layer thickness h and semi-infinite bottom layer.

Top layer/bottom layer materials	**Thermal conductivity of top layer [W m^{-1} K^{-1}]**	**Thermal conductivity of bottom layer [W m^{-1} K^{-1}]**
Ecoflex/Ecoflex	0.22±0.01	0.22±0.01
Ecoflex/Sylgard 567	0.23±0.01	0.29±0.01
Ecoflex/Sylgard 170	0.21±0.01	0.42±0.02
Ecoflex/Sylgard 164	0.23±0.01	0.66±0.01
Sylgard 567/Ecoflex	0.32±0.01	0.21±0.02
Sylgard 567/Sylgard 567	0.30±0.01	0.30±0.02
Sylgard 567/Sylgard 170	0.30±0.01	0.46±0.02
Sylgard 567/Sylgard 164	0.31±0.01	0.67±0.01

Table S1. Measured thermal conductivity of the double layered materials in Figure 4f. Literature reported thermal conductivity $k_{Sylgard\ 567}$ in range of 0.29-0.3 W m^{-1} K^{-1}[3,4], $k_{sylgard170}$ in range of 0.36-0.48 W m^{-1} K^{-1}[5,6], $k_{sylgard}$ 164 is 0.64 W $m^{-1}K^{-1}$[7].

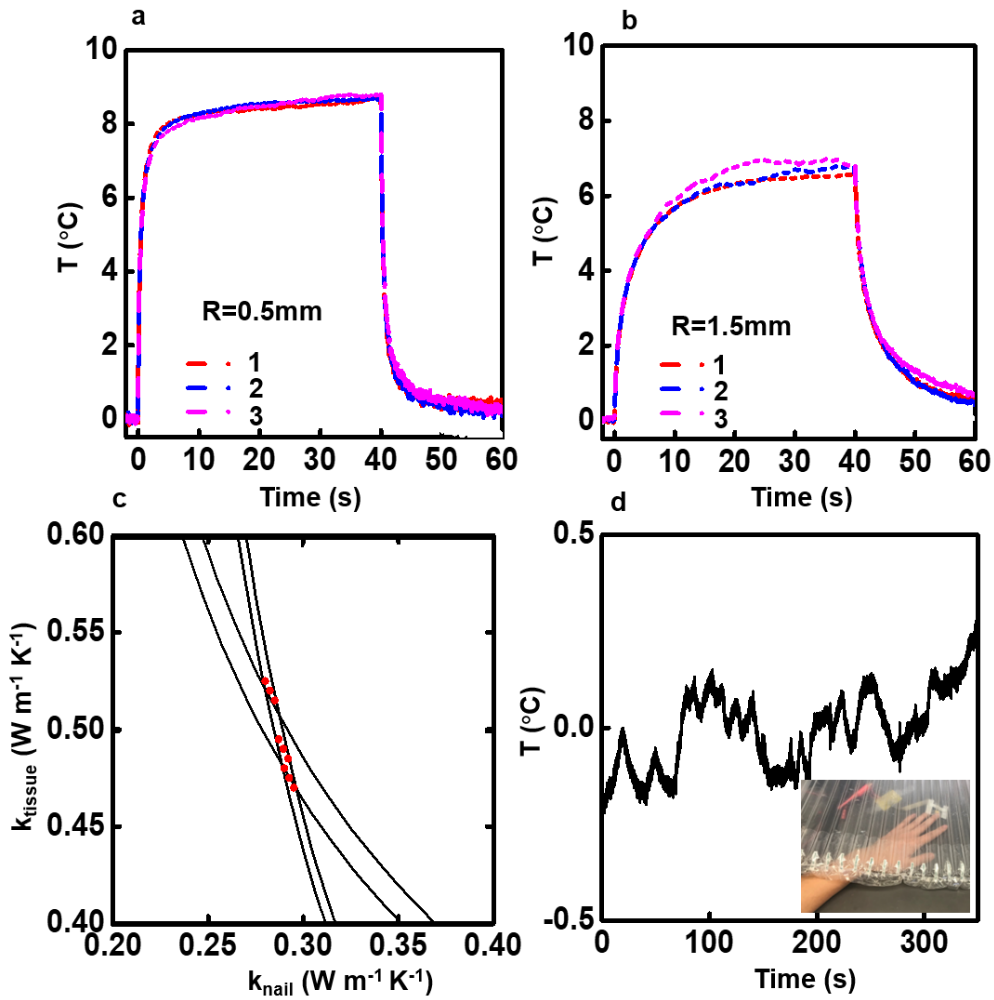

Figure S5. Thermal characterization of the fingernail. (a) Temperature response of a sensor with R=0.5 mm and (b) R=1.5 mm on a test subject (female, 29 years old). Red, blue, purple curves are measured at the same location. (c) FEA fitteresults from the measurements in (a) and (b), with fitted thermal conductivity, k_{nail} and k_{tissue} presented as red points in the area enclosed by minimum and maximum temperature contour lines. (d) Variation in surface temperature of the fingernail measured using a sensor with R=1.5 mm with plastic foam enclosure, as shown in the inset.

In vivo test on human subjects exhibit more temperature fluctuations compared with the in vitro study with petri dish cover. Those fluctuations in the thermal sensor measurement are shown in Figure S5a to c. The deviations between the steady state temperature T_{ss} of each curve is generally 0.3-0.5 °C, in agreement with other literatures.[8,9] The fitted values of k_{nail} and k_{tissue} in Figure S5c reflect influence of the temperature fluctuation. Figure S5 d shows the nail surface temperature fluctuation measured by the R=1.5 mm sensor, as result of summated effects of internal heart production and heat transfers between the body and ambient environment. To reduce the rate of convective heat transfer to the ambient, a plastic foam enclosure covered the subjects' hand without contacting the fingernail.

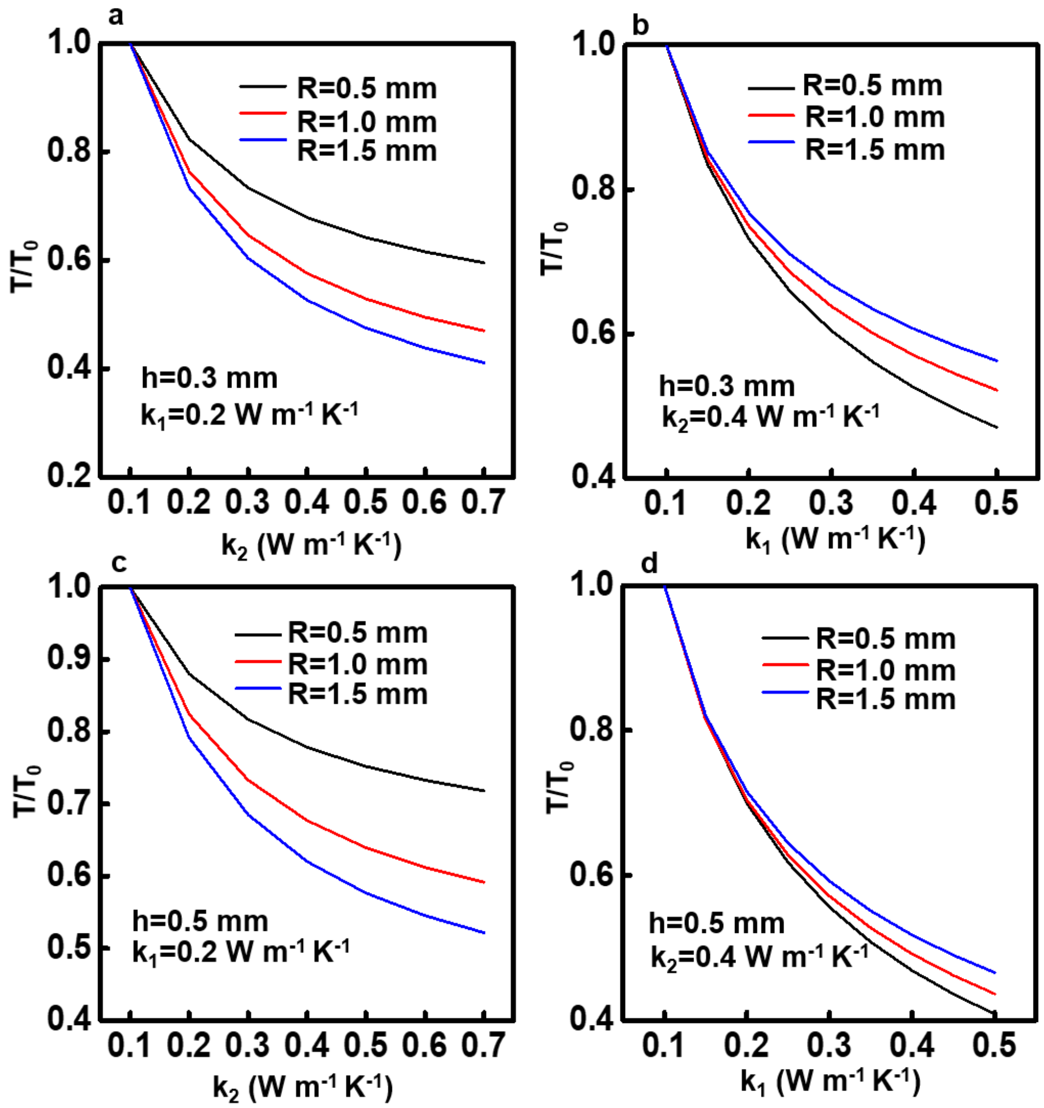

Figure S6. Temperature responses for sensors with different sizes calculated by FEA for the case of a bilayer system. (a) Normalized temperature responses as function of the thermal conductivity of the bottom layer. The radii of the sensors are 0.5, 1.0 and 1.5 mm, and the thickness of the top plate is h=0.3 mm and (c) 0.5 mm, with k_1=0.2 W m^{-1} K^{-1}. (b) Normalized temperature responses as function of the thermal conductivity of the top layer. The radii of the sensors are 0.5, 1.0, 1.5 mm, and the thickness of the top plate is h=0.3 mm and (d) 0.5 mm, with k_2=0.4 W m^{-1} K^{-1}.

Figure S6 summarizes data that reveal the dependence of the response on sensor size. Panel (a) and (c) show that for a fixed top layer, the change of the normalized temperature, T/T_0 (T_0 is the temperature of each sensor with $k_1(k_2)$=0.1 W $m^{-1}K^{-1}$) is larger for the large sensor (R=1.5 mm) than for the small sensor (R=0.5 mm) for both thicknesses of the top layer (h=0.3 mm and 0.5 mm). These results indicate that the larger sensors are more sensitive to the properties of the bottom layer. The small sensors are more sensitive to the top layer as demonstrated in (b) and (d), with bottom layer fixed, the normalized temperature curves show more variation to the top layer thermal conductivity changes for R=0.5 mm than R=1.5 mm sensor.

References

[1] D. T. Dias, A. Steimacher, A. C. Bento, A. M. Neto, M. L. Baesso, *Photochem. Photobiol.* **2007**, *83*, 1144.

[2] M. L. Cohen, *J. Invest. Dermatol.* **1977**, *69*, 333.

[3] SYLGARD® 567 PRIMERLESS SILICONE ENCAPSULANT KIT. Dow Corning, **1999**

[4] *SYLGARD® 567 PRIMERLESS SILICONE ENCAPSULANT KIT*. Dow Corning, **2017**

[5] *SYLGARD® 170 SILICONE ELASTOMER KIT*. Dow Corning, **2017**

[6] *Dow Corning Sylgard 170 Silicone Encapsulant Black*. Dow Corning, **2015**

[7] *SYLGARD® 164 SILICONE ELASTOMER KIT*. Dow Corning, **2015**

[8] H. A. M. Daanen, J. Koedam, S. S. Cheung, *Eur. J. Appl. Physiol.* **2012**, *112*, 2595.

[9] Y. Liu, L. Wang, J. Liu, Y. Di, *J. Therm. Biol.* **2013**, *38*, 440.